

Directed assembly of gold nanoparticle nanowires and networks for nanodevices

Xugang Xiong,^{a)} Ahmed Busnaina,^{b)} Selvapraba Selvarasah, and Sivasubramanian Somu
NSF Nanoscale Science and Engineering Center for High-Rate Nanomanufacturing, Northeastern University, Boston, Massachusetts 02115

Ming Wei and Joey Mead
NSF Nanoscale Science and Engineering Center for High-Rate Nanomanufacturing, University of Massachusetts Lowell, Lowell, Massachusetts 01854

Chia-Ling Chen, Juan Aceros, Prashanth Makaram, and Mehmet R. Dokmeci
NSF Center for High-Rate Nanomanufacturing, Northeastern University, Boston, Massachusetts 02115

(Received 24 March 2007; accepted 2 July 2007; published online 6 August 2007)

Alternating electric field is used to assemble gold nanoparticle nanowires from liquid suspensions. The effects of electrode geometry and the dielectrophoresis force on the chaining and branching of nanowire formation are investigated. The nanowire assembly processes are modeled using finite element calculations, and the particle trajectories under the combined influence of dielectrophoresis force and viscous drag are simulated. Nanoparticle nanowires with 10 nm resolution are fabricated. The wires can be further oriented along an externally introduced flow. This work provides an approach towards rapid assembly and organization of ultrasmall nanoparticle networks. © 2007 American Institute of Physics. [DOI: 10.1063/1.2763967]

One-dimensional (1D) nanoparticle (NP) assemblies are of tremendous significance due to their unique properties in electronic and photonic devices,^{1,2} and the model system they provide to understand fundamental phenomena at the nanoscale.³ However, the realization of anisotropic 1D assembly of NPs remains challenging simply because of the isotropic structure and morphology of NPs.⁴ Templated assembly by using capillary force⁵⁻⁷ or electrophoretic deposition^{8,9} offers many opportunities for the fabrication of ordered arrays. Tang *et al.* developed a template-free strategy to make CdTe particle chains by reducing interparticle repulsion through partial removal of the surface stabilizers,¹⁰ making the van der Waals, chemical and electric-dipole interactions the dominant forces in the formation of 1D particle chains. In addition, the transformation of oriented aggregation of particles into nanowire structures via mutual attachment has been observed for metal and semiconductor NPs.^{11,12} However, most chemically prepared NP assemblies have limited applications for electronic device integrations due to a lack of control of the orientation and length of particle chains. Here, we report an approach using alternating current (ac) electric fields for the fabrication of various particle chain network structures without resorting to further chemical functionalization of NPs or substrates.

Dielectrophoresis (DEP) forces are widely used to manipulate micro- and nanoscale particles.¹³⁻¹⁵ The DEP arises from the polarization of particles in a nonuniform electric field, where the induced dipole moment can be translated into a net force leading to particle movement.¹⁶ The DEP force is proportional to the particle volume as well as the gradient of electric field squared. As a result, the manipulation of smaller particles requires larger field gradients. On the other hand, a higher field gradient may induce convective flow due to heating or electrohydrodynamic effect^{17,18} that

could potentially disturb the dielectrophoretic immobilization of NPs. In addition, the impact of the Brownian motion becomes more evident as the particle size decreases.¹⁹ The controlled assembly of NPs into continuous nanowires of a few nanometers wide and tens of microns long by using DEP is a promising but rarely explored area.

The micro- and nanoelectrodes for the DEP assembly are prepared with standard optical lithography and electron-beam lithography on a 500 nm thick insulating thermal oxide layer. A gold nanoparticle suspension, supplied by BBI International (Cardiff, UK), is used as is. For the dielectrophoresis, a function generator is operated at a frequency between 10 kHz and 1 MHz and a peak-to-peak voltage (V_{p-p}) of 4–10 V. After the ac power is switched on, a droplet (2–3 μ l) suspension of gold NPs is applied onto the chip using a microsyringe. After 2 min of assembly, the droplet is gently blown off by a stream of nitrogen gas, and the power is then switched off.

Figure 1 shows the effects of ac fields on the organization of NP assembly. When the ac field is off, the particles are uniformly dispensed and well separated. When an ac voltage with 1 MHz frequency is applied, NP chain network structures start to form, and most individual particles are linked together. Rather than forming agglomerated micro-wire structures as reported by other groups,²⁰⁻²² we observed that the NPs are assembled into nanowires of a few nanometers wide. By designing electrodes with sharp corners, we introduce strong electric field gradients that are required to selectively control the growth sites of the NP wires. Figure 1(c) shows that dendrite nanowires are preferentially grown from a sharp corner of one electrode and toward the direction of an opposing counterelectrode. However, when the ac frequency is reduced to 10 kHz, no chaining structures are formed. Instead, the particles are mostly assembled on the edge of the electrode with short-range NP agglomerations protruding outward at sharp corners [see Fig. 1(d)]. It has been reported that by reducing the frequency of an applied ac

^{a)}Electronic mail: xiong@coe.neu.edu

^{b)}Electronic mail: busnaina@coe.neu.edu

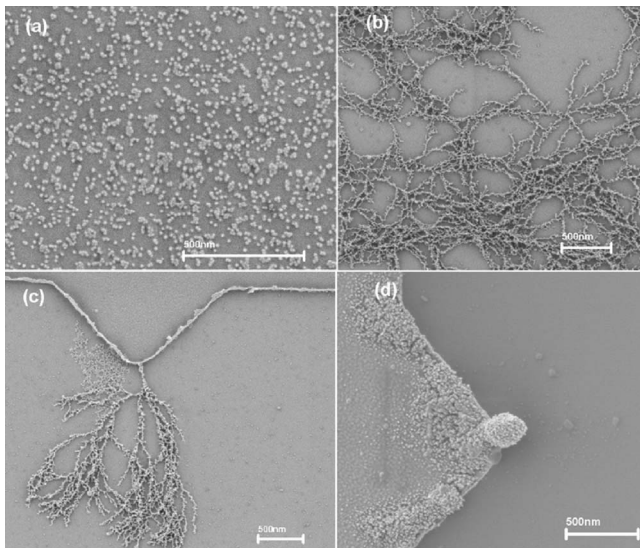


FIG. 1. Effect of ac fields on the reorganization of gold NP network structures. (a) No ac field, (b) ac voltage of $10 V_{p-p}$ applied at 1 MHz. (c) and (d) are NP structures formed at ac frequencies of 1 MHz and 10 kHz, respectively $10(V_{p-p})$. The scale bar in all figures is 500 nm.

voltage from megahertz to kilohertz range, large clusters of particles are usually assembled around opposing electrodes, and it was also reported that increasing the frequency to 1 MHz results in narrow and highly oriented nanowires of less than 100 nm in diameter.²³

For electrode pair with gaps of $10 \mu\text{m}$ and above, the NP wires can be effectively assembled from both ac and grounded sides of the electrodes. NP lines can also grow from different corners of the same electrode as long as the field gradient is high enough due to geometrical configuration [see Figs. 2(a) and 2(b)]. Such a phenomenon indicates that NP wires do not necessarily only bridge two separate opposing electrodes. When the gap between the ends of two approaching particle wires reduces to the diameter of a single particle, the last particle is subject to the attraction forces from both ends and tends to bridge both wires. We also observed that the NP wire growth can be controlled by the application of an external flow. Figures 2(c) and 2(d) show

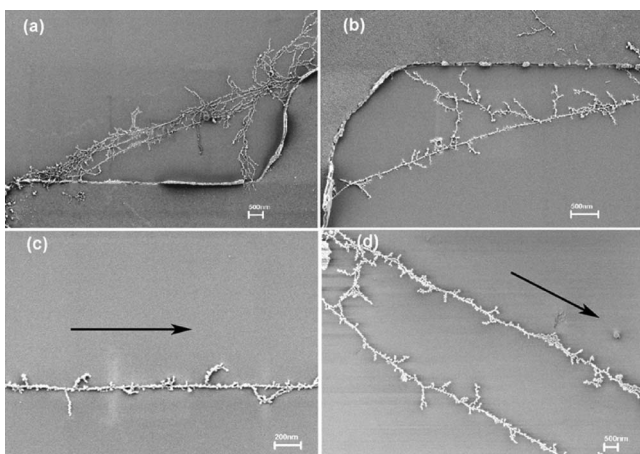


FIG. 2. Effect of electrode geometry and flow direction on the organization of NP wires. [(a) and (b)] Gold particle nanowire formation around corner areas of only one electrode. (c) and (d) show that the nanowires are oriented along the flow direction. The scale bar in (a), (b), and (d) is 500 nm, and 200 nm in (c).

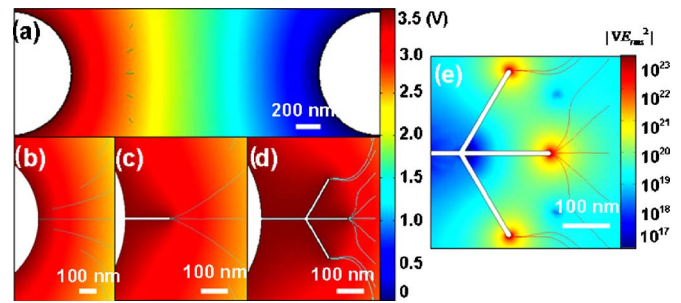


FIG. 3. Simulation results showing particle trajectories under the combined influence of DEP and viscous drag forces. (a) shows the potential plot with a set of particles moving short distances from their initial location, (b)–(d) show the potential contour plot with particle trajectories at growth stages 1–3, and (e) plot of ∇E_{rms}^2 around a three branched nanowire domain.

that the NP wires are stretched and aligned along the applied flow. This flow is induced by a nitrogen jet that directs the particle wires to follow the desired direction as shown. The results also show that the dielectrophoretically assembled gold NPs have formed good interparticle bonds that are not easily separated or broken by the flow.

The application of an ac field produces a time-dependent polarization of dipoles in particles. The resulting dielectrophoretic force is given by¹⁶

$$F_{\text{DEP}} = 2\pi\epsilon_m \text{Re}[K(\omega)]a^3 \nabla E_{\text{rms}}^2, \quad (1)$$

where ϵ_m is the dielectric constant of medium, a is the particle radius, ω is the angular field frequency, and E_{rms} is the root-mean-square electric field. The direction of the force is determined by the sign of $\text{Re}[K(\omega)]$, the real part of Clausius-Mossotti factor, given by¹⁶

$$\text{Re}[K(\omega)] = \frac{\epsilon_p - \epsilon_m}{\epsilon_p + 2\epsilon_m} + \frac{3(\epsilon_m\sigma_p - \epsilon_p\sigma_m)}{\tau_{\text{MW}}(\sigma_p + 2\sigma_m)^2(1 + \omega^2\tau_{\text{MW}}^2)}, \quad (2)$$

where ϵ is the permittivity and σ is the conductivity, and the subscripts p and m denote particle and medium, respectively. $\tau_{\text{MW}} = (\epsilon_p + \epsilon_m)/(\sigma_p + 2\sigma_m)$ is the time constant that characterizes the decay of a dipolar distribution of charge on the surface of a spherical particle. For metallic particles, $\text{Re}[K(\omega)]$ is ~ 1 when $\omega\tau_{\text{MW}} \ll 1$. The particle dendrite formation can be modeled by simulating the particle trajectories under the combined influence of dielectrophoretic force and opposing viscous drag. COMSOL multiphysics modeling software is used to simulate the potential contour for a typical micro-electrode configuration. The gradient of the electric field square ∇E_{rms}^2 is used to calculate the dielectrophoretic force.

Different stages of the NP wire assembly are simulated by tracing the particle movement under the combined effect of DEP force and opposing viscous drag. Initially, the particles are being attracted towards the protruding electrode end, as shown in Figs. 3(a) and 3(b). Figure 3(a) shows that the NPs move a short distance from their initial locations. Similar locations are used in Figs. 3(b)–3(e). Once the first particle assembles on the electrode [stage 1, Fig. 3(b)], it becomes a part of the electrode and the electric field will be enhanced to favor a continual chaining formation. As shown in Fig. 3(c), stage 2 starts when a short NP wire has assembled. The nearby particles are preferentially redirected towards the far end of the nanowire for the wire to grow. Depending on the approaching angle and direction, some

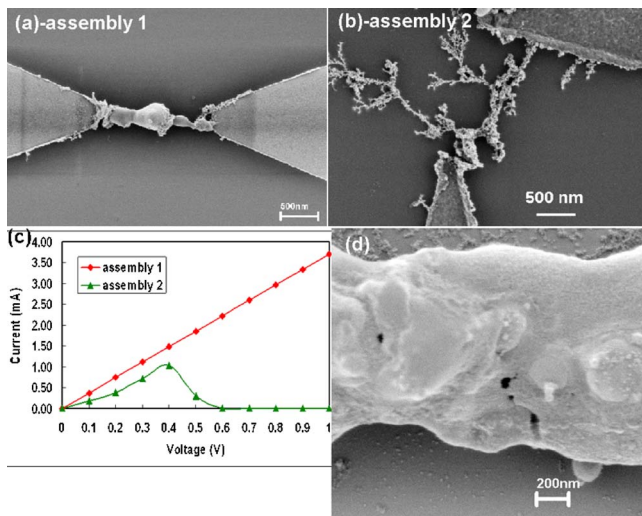


FIG. 4. Characterization of typical DEP assembled gold nanoparticle structures between different electrodes. (a) fused or melted nanoparticle interconnect, (b) half-melted/unmelted nanoparticle interconnect, (c) I - V characterization of nanoparticle interconnect from (a) to (b), and (d) high resolution image of a typical fused nanoparticle interconnect structure. The scale bar in (a) and (b) is 500 nm, and 200 nm in (d).

NPs can be attached to either or both sides of the nanowire end, and dendrite structures can be formed. Depending on the local particle concentration with respect to the protruding ends of the nanowires, the number of particles assembled to the nanowire ends may vary, as displayed in Fig. 3(d) (stage 3). As a result, the growing speeds of the branched nanowires may also vary. In our case, both experimental results and simulation show that the growth of a central NP wire is favored. Figure 3(e) shows the plot of ∇E_{rms}^2 for the condition of stage 3. The simulation indicates that the highest field gradients occur near the tips of an electrode. In order to assemble ultrasmall particles, the sharp corner design is usually required.

We further measured the current-voltage (I - V) characteristics of the two assembled gold NP structures between electrodes, as shown in Figs. 4(a) and 4(b) using an HP 4155A parameter analyzer. The measured resistance is the sum of the resistance due to the fabricated micron scale electrodes R_{elec} and that of the assembled nanoparticle interconnects R_{part} . We fabricated electrodes identical to the one used in the assembly but without a gap (typically where the assembly takes place) and measured their resistance R_{elec} as a reference. The values of the reference resistance are used to give an approximate R_{elec} , which will help in estimating R_{part} . The electrode resistance R_{elec} is $\sim 200 \Omega$ for the electrode used in assembly 1 and $\sim 20 \Omega$ for the electrode used in assembly 2. If we deduct the electrode resistance R_{elec} from the measured nanowire resistance for both assemblies, we get $R_{\text{part}} \sim 500 \Omega$ for the half-fused nanoparticle nanowire and $\sim 70 \Omega$ for the fused nanoparticle nanowire.

Our other experimental results have also consistently shown low electrical resistance of gold nanoparticle assembled structures (40–120 Ω for three dimensional nanodevices²⁴), in the form of half-melted Au nanoparticle structures. Compared with the reported resistance values in

the literature,^{7,25} we obtained a relatively lower Ohmic behavior of the NP bridges. High resolution field effect scanning electron microscopy (FESEM) image [in Fig. 4(d)] has shown a detailed surface profile of a typical melted or fused Au nanoparticle structure. Once the bridges are formed, individual particles become unresolvable and they fuse into much wider and thicker structures with a relatively smooth surface. A potential explanation for the low Ohmic resistance of these melt-solidified structures might be that the initial interparticle and particle-electrode contact resistances are reduced due to this melting effect.

In summary, we have shown that by using micro- and nanoelectrodes, we can dielectrophoretically assemble NP wires of a few nanometers wide and microns long. Complex chaining and dendrite nanowire networks are assembled by varying the electrode design. Multiphysics modeling of the NP assembly trajectories provides an insight into the complex growth mechanism of the nanowires. This work can be extended to yield large scale production of extremely small nanowires that would potentially enable interconnection in high-performance nanoelectronics applications.

This work was supported by the National Science Foundation Nanoscale Science and Engineering Center (NSEC) for High-rate Nanomanufacturing (NSF Grant No. 0425826).

- ¹S. A. Maier, M. L. Brongersma, P. G. Kik, S. Meltzer, A. A. G. Requicha, and H. A. Atwater, *Adv. Mater.* (Weinheim, Ger.) **13**, 1501 (2001).
- ²S. A. Maier, P. G. Kik, H. A. Atwater, S. Meltzer, E. Harel, B. E. Koel, and A. A. G. Requicha, *Nat. Mater.* **2**, 229 (2003).
- ³A. N. Shipway, E. Katz, and I. Willner, *ChemPhysChem* **1**, 18 (2000).
- ⁴Z. Tang and N. A. Kotov, *Adv. Mater.* (Weinheim, Ger.) **17**, 951 (2005).
- ⁵Y. Yin, Y. Lu, B. Gates, and Y. Xia, *J. Am. Chem. Soc.* **123**, 8718 (2001).
- ⁶F. Juillerat, H. H. Solak, P. Bowen, and H. Hofmann, *Nanotechnology* **16**, 1311 (2005).
- ⁷Y. Cui, M. T. Bjork, J. A. Liddle, C. Sonnichsen, B. Boussert, and A. P. Alivisatos, *Nano Lett.* **4**, 1093 (2004).
- ⁸E. Kumacheva, R. K. Golding, M. Allard, and E. Sargent, *Adv. Mater.* (Weinheim, Ger.) **14**, 221 (2002).
- ⁹X. Xiong, P. Makaram, A. Busnaina, K. Bakhtari, S. Somu, N. McGruer, and J. Park, *Appl. Phys. Lett.* **89**, 193108 (2006).
- ¹⁰Z. Tang, N. A. Kotov, and M. Giersig, *Science* **297**, 237 (2002).
- ¹¹M. Giersig, I. Pastoriza-Santos, and L. M. Liz-Marzan, *J. Mater. Chem.* **14**, 607 (2004).
- ¹²C. Pacholski, A. Kornowski, and H. Weller, *Angew. Chem., Int. Ed.* **41**, 1188 (2002).
- ¹³N. G. Green and H. Morgan, *J. Phys. Chem. B* **103**, 41 (1999).
- ¹⁴I. Tuval, I. Mezić, F. Bottausci, Y. T. Zhang, N. C. MacDonald, and O. Piro, *Phys. Rev. Lett.* **95**, 236002 (2005).
- ¹⁵L. Zheng, S. Li, J. P. Brody, and P. J. Burke, *Langmuir* **20**, 8612 (2004).
- ¹⁶T. B. Jones, *Electromechanics of Particles* (Cambridge University Press, Cambridge, 1995), p. 34.
- ¹⁷M. Trau, D. A. Saville, and I. A. Aksay, *Langmuir* **13**, 6375 (1997).
- ¹⁸K. H. Bhatt, S. Grego, and O. D. Velev, *Langmuir* **21**, 6603 (2005).
- ¹⁹A. Ramos, H. Morgan, N. G. Green, and A. Castellanos, *J. Phys. D* **31**, 2338 (1998).
- ²⁰K. H. Bhatt and O. D. Velev, *Langmuir* **20**, 467 (2004).
- ²¹S. O. Lumsdon and D. M. Scott, *Langmuir* **21**, 4874 (2005).
- ²²Y. J. Yuan, M. K. Andrews, and B. K. Marlow, *Appl. Phys. Lett.* **85**, 130 (2004).
- ²³R. Kretschmer and W. Fritzsche, *Langmuir* **20**, 11797 (2004).
- ²⁴N. Khanduja, S. Selvarasah, C. Chen, M. R. Dokmeci, X. Xiong, P. Makaram, and A. Busnaina, *Appl. Phys. Lett.* **90**, 083105 (2007).
- ²⁵I. Amlani, A. M. Rawlett, L. A. Nagahara, and R. K. Tsui, *Appl. Phys. Lett.* **80**, 2761 (2006).